Received: 16 November 2022 | Accepted: 2 March 2023

DOI: 10.1002/ppj2.20068

The Plant Phenome Journal OPEN ACCESS

SPECIAL SECTION: NORTH AMERICAN PLANT PHENOTYPING NETWORK (NAPPN) PROC. 2022

Comparison of open-source three-dimensional reconstruction pipelines for maize-root phenotyping

Suxing Liu[1,4] | **Wesley Paul Bonelli**[3] | **Peter Pietrzyk**[1] | **Alexander Bucksch**[1,2,3,4]

[1]Department of Plant Biology, University of Georgia, Athens, Georgia, USA

[2]Warnell School of Forestry and Natural Resources, University of Georgia, Athens, Georgia, USA

[3]Institute of Bioinformatics, University of Georgia, Athens, Georgia, USA

[4]School of Plant Sciences, University of Arizona, Tucson, Arizona, USA

Correspondence
Alexander Bucksch, School of Plant Sciences, University of Arizona, Tucson, AZ 85721, USA.
Email: bucksch@arizona.edu

Assigned to Associate Editor David Ertl.

Funding information
National Science Foundation, Grant/Award Number: 1845760; Advanced Research Projects Agency - Energy, Grant/Award Number: DE-AR0000821

Abstract

Understanding three-dimensional (3D) root traits is essential to improve water uptake, increase nitrogen capture, and raise carbon sequestration from the atmosphere. However, quantifying 3D root traits by reconstructing 3D root models for deeper field-grown roots remains a challenge due to the unknown tradeoff between 3D root-model quality and 3D root-trait accuracy. Therefore, we performed two computational experiments. We first compared the 3D model quality generated by five state-of-the-art open-source 3D model reconstruction pipelines on 12 contrasting genotypes of field-grown maize roots. These pipelines included COLMAP, COLMAP+PMVS (Patch-based Multi-View Stereo), VisualSFM, Meshroom, and OpenMVG+MVE (Multi-View Environment). The COLMAP pipeline achieved the best performance regarding 3D model quality versus computational time and image number needed. In the second test, we compared the accuracy of 3D root-trait measurement generated by the Digital Imaging of Root Traits 3D pipeline (DIRT/3D) using COLMAP-based 3D reconstruction with our current DIRT/3D pipeline that uses a VisualSFM-based 3D reconstruction on the same dataset of 12 genotypes, with 5–10 replicates per genotype. The results revealed that (1) the average number of images needed to build a denser 3D model was reduced from 3000 to 3600 (DIRT/3D [VisualSFM-based 3D reconstruction]) to around 360 for computational test 1, and around 600 for computational test 2 (DIRT/3D [COLMAP-based 3D reconstruction]); (2) denser 3D models helped improve the accuracy of the 3D root-trait measurement; (3) reducing the number of images can help resolve data storage problems. The updated DIRT/3D (COLMAP-based 3D reconstruction) pipeline enables quicker image collection without compromising the accuracy of 3D root-trait measurements.

1 | INTRODUCTION

Root phenotyping is essential in research projects aiming to improve water uptake, nitrogen capture, and carbon sequestration (Ault, 2020; Lynch, 2019; Lynch & Wojciechowski, 2015; Paustian et al., 1997; Smith et al., 2007). However, advanced methods are required to measure and quantify complex root architectures in the field environment.

With the development of computer vision techniques, image-based root phenotyping with consumer cameras has emerged as a cost-efficient, highly scalable, and accessible alternative to expensive high-end imaging devices. Established 2D image-based root-phenotyping methods, such as digital imaging of root traits (DIRT) (Bucksch et al., 2014), archiDART (Delory et al., 2016), EZ-Root-VIS (Shahzad et al., 2018), GiA Roots (Galkovskyi et al., 2012), and RhizoVision (Seethepalli et al., 2020) provide highly accurate trait measurements. However, 2D imaging approaches can only capture partial information from dense and highly occluded 3D maize-root architectures. Quantifying important traits, such as crown root number and whorl number, and their distances remains challenging.

The use of 3D imaging techniques in root phenotyping is promising because of their ability to leverage multiple views of a given scene to resolve occlusion in dense root architectures (Bucksch, 2014; Clark et al., 2011; Dowd et al., 2022; Topp et al., 2013). However, 3D imaging methods, such as X-ray CT (Shao et al., 2021) or magnetic resonance imaging (MRI; van Dusschoten et al., 2016), are 100–1000 times more expensive than multicamera systems (Liu et al., 2021), and do not meet the needs of large-scale field studies due to the high operation cost and difficulties in deploying in the field environment. Moreover, 3D imaging methods incur labor costs for highly trained staff and custom-shielded rooms for operations. Therefore, X-ray CT and MRI techniques are unsuitable for capturing root architecture with high throughput. In contrast, multicamera systems can scale at a fraction of the cost of 3D imaging methods and require neither highly trained staff nor custom facilities for their operation.

Fortunately, open-source image-based 3D reconstruction pipelines (Table 1) like COLMAP (Schonberger & Frahm, 2016), COLMAP+PMVS (Furukawa & Ponce, 2007), VisualSFM (Wu, 2011), Meshroom (Griwodz et al., 2021), and OpenMVG+MVE (Fuhrmann et al., 2014; Moulon et al., 2016) enable 3D reconstructions of root system architectures from large sets of unordered images obtained using multicamera systems (Hoppe et al., 2012; Liu et al., 2021).

Despite the availability of highly developed reconstruction pipelines, to our knowledge, performance on 3D root reconstruction tasks has not previously been quantified. Until now, relationships between model quality, image count, and computation time have not been thoroughly explored, and it has remained unclear whether the model quality sufficient for detailed analysis of root traits is possible without significant performance penalties.

Core Ideas

- 3D reconstruction quality faces a trade-off between number of images and computation time.
- Increasing computation time reduces the human factor in root trait measurement.
- Optical 3D root phenotyping is an economical, highly scalable, and automated high-throughput solution.

To answer the question above, we performed two computational experiments. We compared the 3D model quality generated by the above five open-source 3D model reconstruction pipelines on 12 samples from 12 contrasting genotypes of field-grown maize roots in the first computational experiment. The 3D model quality comparison included visual quality, number of points and surface density of a 3D point cloud model, and computation time. The COLMAP pipeline achieved the best performance regarding 3D model quality, which represents the best-observed tradeoff between the point cloud metrics number of points and surface density, image number, and runtime. In the second computational experiment, we implemented COLMAP in the 3D reconstruction pipeline in DIRT/3D (Liu et al., 2021) and compared the accuracy of 3D root traits generated by DIRT/3D (COLMAP-based 3D reconstruction) pipeline with our current DIRT/3D (VisualSFM-based 3D reconstruction) pipeline from the same dataset, including 12 genotypes with 5–10 replicates per genotype (Liu et al., 2021). For brevity, we shall now refer to DIRT/3D (COLMAP-based 3D reconstruction) pipeline as DIRT/3D (COLMAP), and DIRT/3D (VisualSFM-based 3D reconstruction) pipeline as DIRT/3D (VisualSFM).

In the following section, we discuss the methodology including root sample collection, two computational experiments, and the statistical analysis method. Then, we visually and quantitatively assess the quality of trait measurements from reconstructed models of maize genotypes.

2 | MATERIALS AND METHODS

2.1 | Root sample collection

We used the same root samples as described in Liu et al. (2021), including 12 genotypes with 5–10 replicates per genotype. The plants were grown at Pennsylvania State University's Russell E. Larson Agricultural Research Center, which has Hagerstown silt loam soil (fine, mixed, semi-active,

TABLE 1 Feature comparison of open-source pipelines for image-based 3D reconstruction.

Pipeline name	Pipeline feature highlights	Project website
COLMAP v3.7	Improvements over VisualSFM: Scene graph augmentation, next best view selection, robust and efficient triangulation, an iterative bundle adjustment, retriangulation, and outlier filtering strategy.	https://demuc.de/colmap/
COLMAP v3.7 + PMVS	Use of patch-based multi-view stereo to improve the dense reconstruction of COLMAP.	https://www.di.ens.fr/pmvs/ https://demuc.de/colmap/
VisualSFM	VisualSFM is likely the most popular structure from Motion method. It uses GPU supported scale-invariant features transform (SIFT) and model-based bundle adjustment to reconstruct 3D point clouds from unordered photo collections.	http://ccwu.me/vsfm/
Meshroom	Meshroom obtains high dynamic range images by stitching multiple low dynamic range images into a panorama to estimate the motion of a moving camera.	https://alicevision.org/
OpenMVG+MVE	Feature matching uses ANN-kD trees or cascade hashing instead of SIFT strategies used in VisualSFM.	https://github.com/openMVG/openMVG

mesic Typic Hapludalf). The selected genotypes represent extremes of dense versus sparse, large versus small, and maximum and minimum number of whorls selected from a full diversity panel. The 12 genotypes included six inbred lines (B101, B112, DKIB014, LH123HT, Pa762, and PHZ51) and six hybrid lines (DKPB80 × 3IIH6, H96 × 3IIH6, LH59 × PHG29, Pa762 × 3IIH6, PHG50 × PHG47, and PHZ51 × LH59). Sampling followed the shovelomics protocol, which minimizes variation by selecting similar representative architectures. Shoots were removed above all root-producing nodes and air-dried on a greenhouse bench. Then, the roots were transported to the lab for imaging.

2.2 | Three-dimensional root-model reconstruction and three-dimensional trait computation

2.2.1 | Computational Experiment 1: Image capture and computational methods

The image collection was conducted in an imaging chamber prototype built for Pennsylvania State University (Shi et al., 2019). Since this imaging chamber was equipped with a higher resolution camera than the cameras described in Liu et al. (2021), we selected 12 roots from all the samples, with each root representing one genotype. We captured images of each root using this prototype imaging chamber, as conceptually introduced in Shi et al. (2019). The images were captured using 10 cameras (Image Source DFK 33ux183 USB 3.0, 12 mm focal length V1228-MPY2 12 Megapixel Machine Vision Lens) arrayed around a central focal point. Image capture was synchronized using a cluster of 10 Raspberry Pi 4s with a server-client design. For each sample, approximately 360 images with an image resolution of 5,472 × 3,648 were taken. The number of images was chosen after evaluating the scanning geometry of this 3D scanner following the method described in Liu et al. (2009). We obtained an upper bound of the number of images needed to avoid under-sampling of the multi-view scanning setup. Blurred images, which were caused by motion blur effect due to the rotation of all cameras, were manually removed from the datasets.

We captured 12 sets of images. Then, we computed 60 3D root models with the five 3D reconstruction pipelines (COLMAP, COLMAP+PMVS VisualSFM, Meshroom, and OpenMVG+MVE). The 3D root-trait measurement was conducted using the same pipeline as that described in Liu et al. (2021).

2.3 | Computational environment

We conducted the firitst computational experiment on a DELL workstation. (OptiPlex 7080, 10th Generation Intel Core i9-10900K, 20 MB Cache, 10 Cores, 20 Threads, 3.7 GHz–5.3 GHz, 125 W, 64 GB RAM, 4 × 16 GB, DDR4, M.2 2280, 1 TB hard drive, Gen 3 PCIe x4 NVMe, Class 40 SSD). In addition, we used graphics processing units (GPU) to facilitate the computation of the software-supported GPUs. The GPU model with the DELL workstation was a GeForce RTX 2070 SUPER, NVIDIA Corporation TU104, nvcc: NVIDIA (R) Cuda compiler driver. All the pipelines were tested under the command-line interface to generate related 3D root models in point cloud format. The scripts are on GitHub (https://github.com/Computational-Plant-Science/3D_review_scripts/tree/master, folder Computational_test_1).

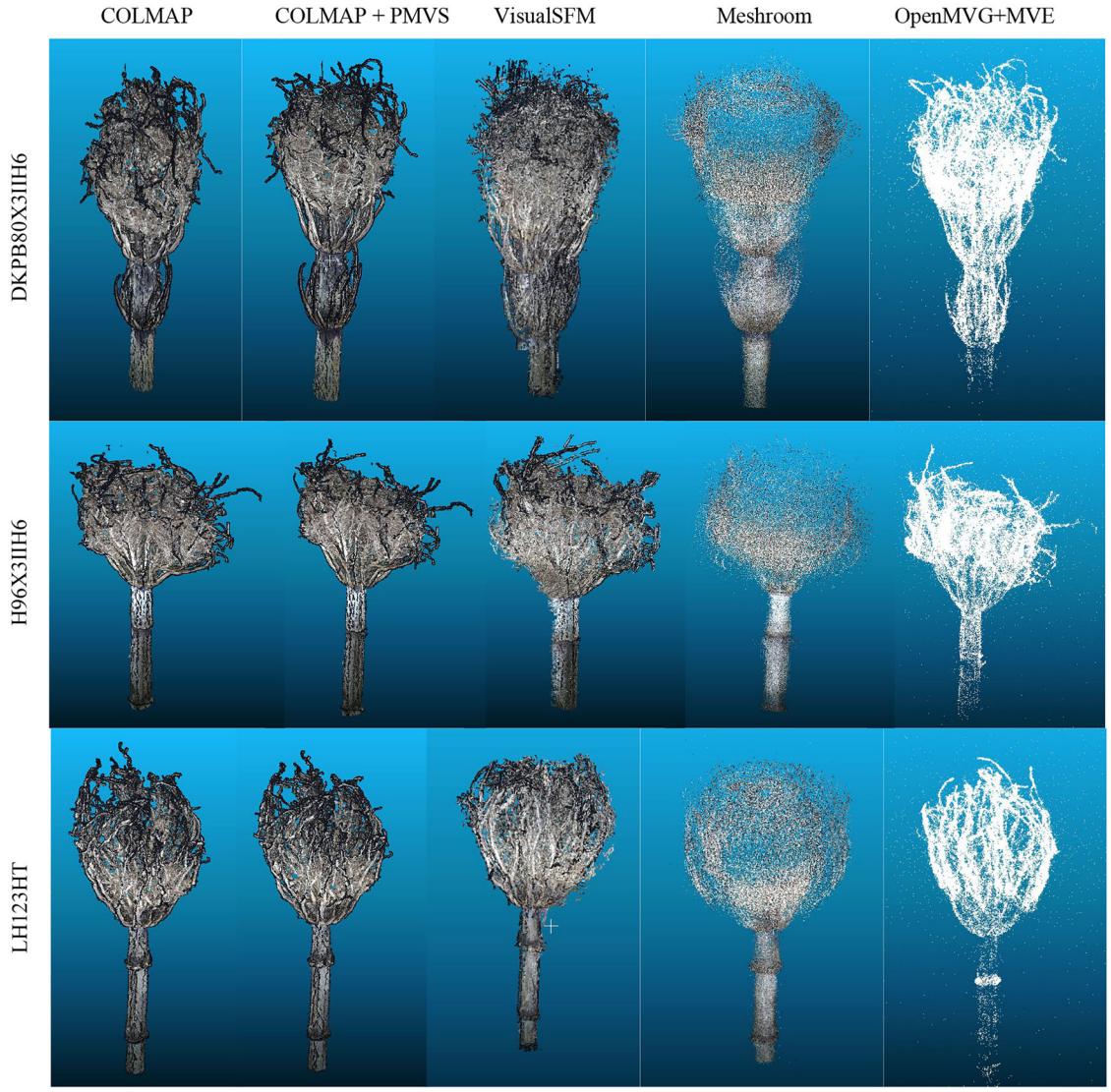

FIGURE 1 Visual comparison of three reconstructed maize genotypes. The 3D root models in each row compare the same genotype across different 3D reconstruction pipelines. The 3D root models in each column compare a 3D reconstruction pipeline across different genotypes.

2.4 | Computational Experiment 2: Image capture and computational methods

For each root sample, we used around 600 images captured with the 3D scanner described in Liu et al. (2021). Each image has a resolution of 3856 × 2764 pixels, which is about half the resolution used in Computational Experiment 1. We evaluated the scanning geometry of the 3D scanner to obtain an estimate of the number of images needed to avoid under-sampling of the multi-view scanning setup as described in Liu et al. (2009). As a result, we chose 600 images as a practical and feasible number of images. Blurred images, which were caused by motion blur effect due to the rotation of all cameras, were manually removed from the datasets.

We computed 80 3D root models for the 12 genotypes with DIRT/3D (COLMAP). The 3D trait measurement of the roots was conducted using the same pipeline as that described in Liu et al. (2021).

2.5 | Computational environment

The computation was conducted on the high-performance-computing (HPC) resource SAPELO2 at the Georgia Advanced Computing Resource Center (GACRC). We ran DIRT/3D (COLMAP) in a singularity container and recorded the running time for each execution of the container. The singularity container was retrieved from https://hub/docker.com/r/computationalplantscience/dirt3d-reconstruction and https://hub.docker.com/r/computationalplantscience/dirt3d-traits. All the scripts for this computational experiment are available on GitHub

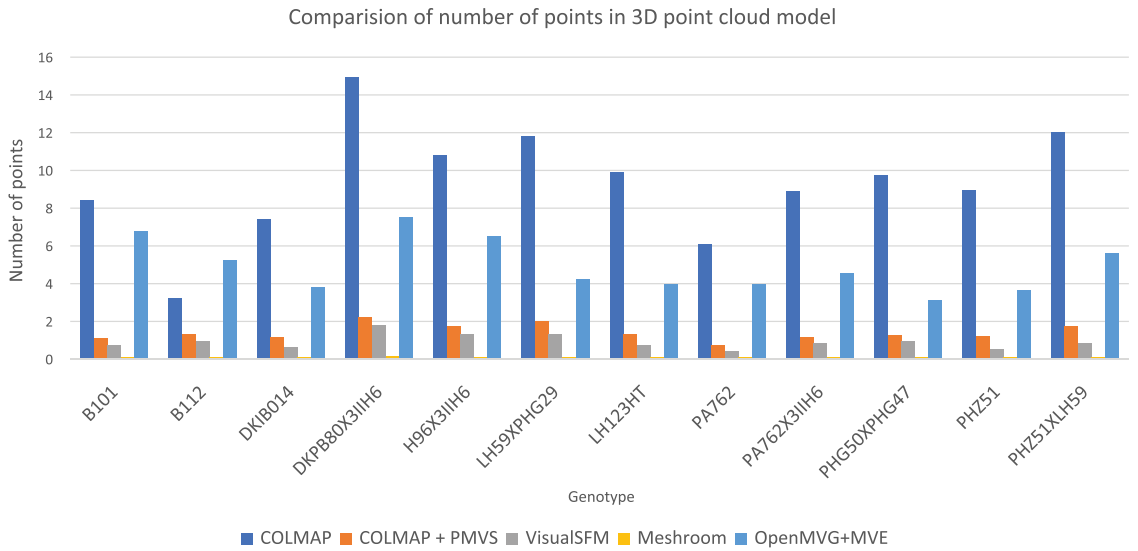

FIGURE 2 Comparison of the number of points in 3D models. The five pipelines are color labeled, and the lengths of bars represent the value of the number of points in each 3D point cloud model.

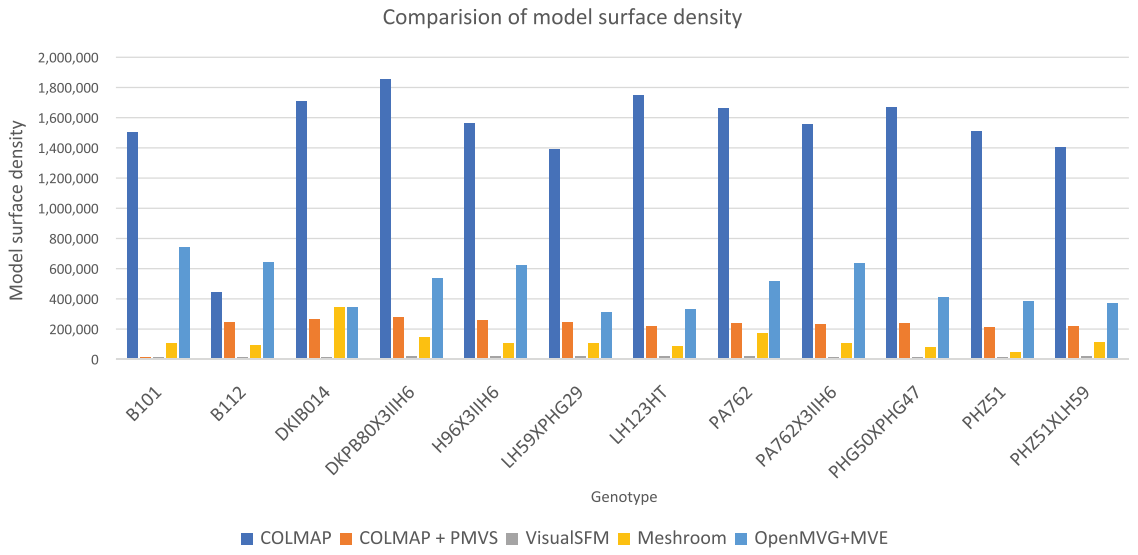

FIGURE 3 Comparison of surface density of 3D models. COLMAP produced models with the highest surface density among all the pipelines, whereas VisualSFM produced the lowest surface density. The five tested pipelines are color labeled, and the lengths of the bars represent the value surface density of each 3D point cloud model.

(https://github.com/Computational-Plant-Science/3D_review_scripts/tree/master, folder Computational_test_2).

2.6 | Three-dimensional model quality computation

We used CloudCompare v2.12.alpha (Girardeau-Montaut, 2016) to compute the number of points in the 3D point cloud model and to estimate the surface density of a point cloud in computational Experiments 1 and 2. We loaded each point cloud model into CloudCompare v2.12.alpha using the software's graphical user interface. We then retrieved the number of points via the "Properties" tab.

The surface density S was estimated by counting the number of neighbors N inside a sphere of radius R for each point. The surface density S is defined as follows:

$$S = N / \left(\pi \times R^2\right)$$

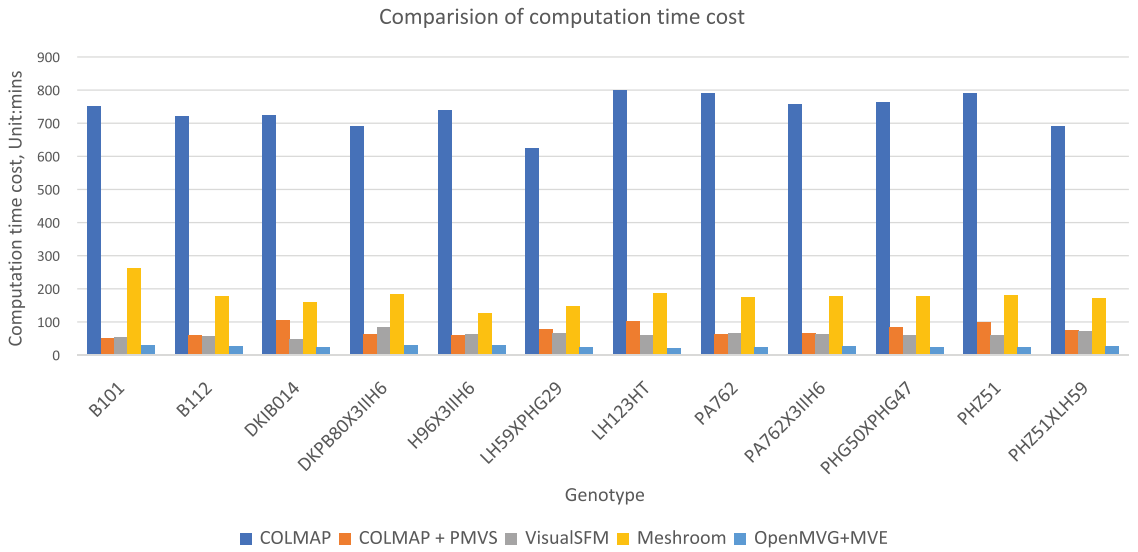

FIGURE 4 Comparison of computation times per 3D reconstruction pipeline. The five tested pipelines are color labeled, and the lengths of the bars represent the time needed to compute the point cloud model. Although COLMAP generated the best 3D models among all the pipelines regarding number of points and surface density, it also took the most computational time, on average. Meshroom was the second most time-consuming pipeline. COLMAP + PMVS took the least computational time, on average.

2.7 | Statistical analysis

The CORREL function in Microsoft Excel (Microsoft 365 A3) and the Analysis ToolPak add-in for Excel were used to compute correlation coefficients between the two sets of trait measurements derived from DIRT/3D (COLMAP) and DIRT/3D (VisualSFM). In addition, the built-in R-squared formula in Microsoft Excel (Microsoft 365 A3) was used to compute the R-squared value in the regression analysis.

3 | RESULTS

3.1 | Computational Experiment 1: Qualitative and quantitative comparison of three-dimensional model quality from five open-source three-dimensional reconstruction pipelines

3.1.1 | Visual assessment

We selected 12 field-grown maize roots from 12 different genotypes to compute 3D point clouds using all five pipelines. For each root sample, around 360 images were captured, and overall, 60 3D point cloud models were generated.

Figure 1 provides a visual comparison of the computed 3D models with the pipelines COLMAP, VisualSFM, OpenMVG, Meshroom, and MVE (Fuhrmann et al., 2014). Among all the tested 3D reconstruction pipelines, COLMAP and COLMAP+PMVS achieved good visual results, in terms of model completeness, with no obvious disconnection of roots or missing parts of the root system. With the reduced image dataset, VisualSFM tended to omit fine details, such as brace roots at the margins of the point cloud. Meshroom produced models with large interior gaps. OpenMVG+MVE displayed finer details than VisualSFM but does not provide color information per point.

3.2 | Quantitative assessment

We assessed the two sets of point cloud metrics (number of points and surface density) for each 3D point cloud model. "Number of points" represents the total of 3D points generated by a 3D reconstruction pipeline. "Surface density" is the average density across the surface of the root architecture. The comparison results for the number of points are illustrated in Figure 2. The COLMAP pipeline produced the largest number of points, achieving, on average, 94 times the number of points of Meshroom, which generated the fewest points. In general, COLMAP outperformed all the other tested pipelines regarding the number of points per root system (Figure 2).

In addition to the number of points, we compared the surface density of the point clouds generated by each pipeline. Higher surface density values are desirable for point cloud characteristics. The comparison of surface density in Figure 3 reveals that COLMAP and OpenMVG+MVE produced the models with the largest surface density in most of the root samples. The surface density generated by COLMAP was, on average, 94 times the surface density generated by VisualSFM, whereas OpenMVG+MVE was 31 times the surface

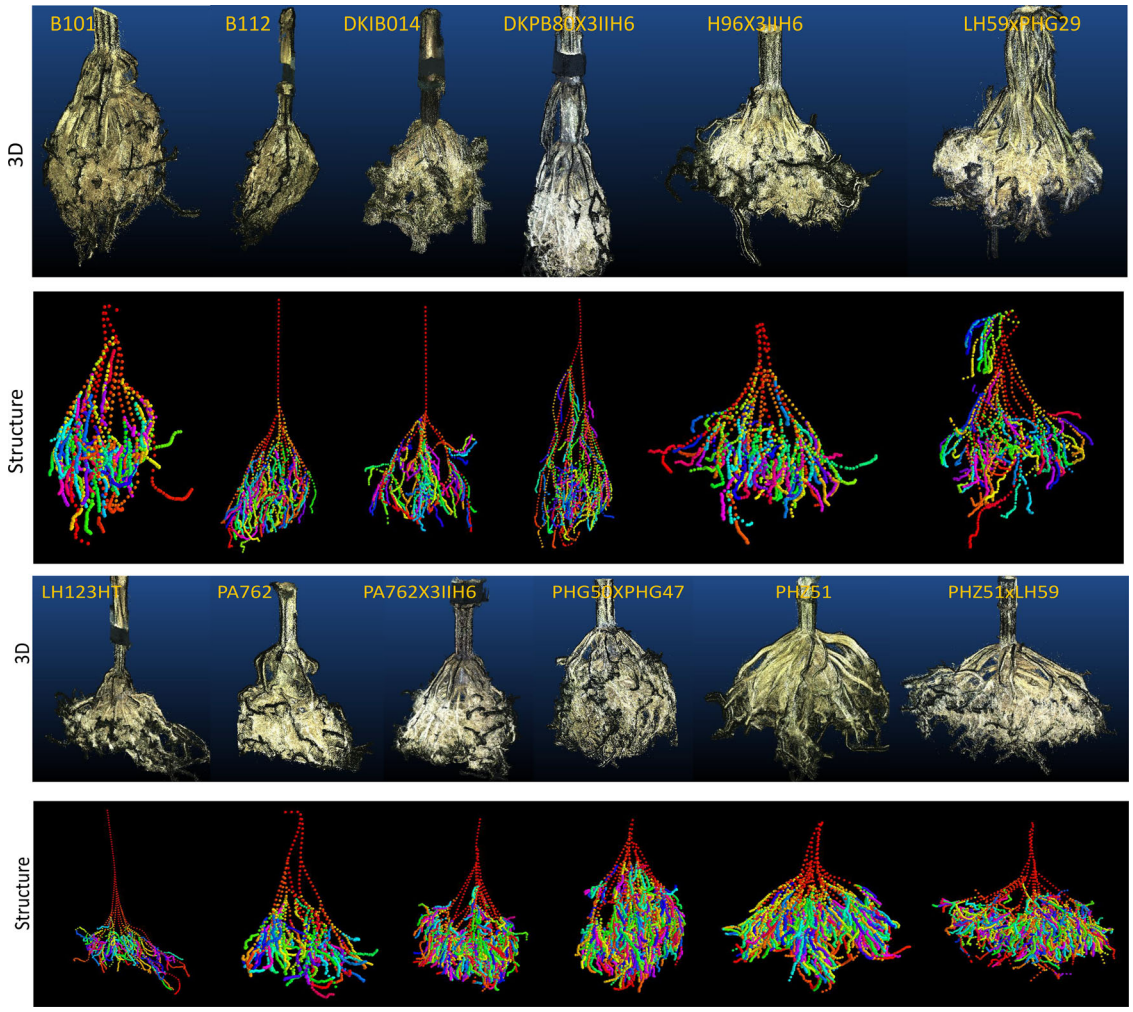

FIGURE 5 12 sample 3D root models and their related computed root structure DIRT/3D (COLMAP). The rows named "3D models" provide examples of the computed 3D root point clouds per genotype. The rows named "Structure" illustrate the computed root architecture representation as skeletal curves.

density of VisualSFM. VisualSFM generated models with the lowest surface density among all the pipelines.

In Computational Experiment 1, COLMAP produced the best 3D model results in terms of the number of points and surface density for most of the root samples. However, we noticed there are exceptions such as genotype B112. This exception can be explained by the physical arrangements of roots within the root system as a discriminating factor between genotypes. As such, different arrangements lead to different degrees of occlusion. Therefore, these root architectures are likely to show potential genotype dependence.

On average, COLMAP computed almost 29 times longer than the quickest algorithm (OpenMVG+MVE), and five times longer than Meshroom. COLMAP+PMVS was significantly faster than COLMAP, and needed, on average, three times longer than OpenMVG+MVE to produce the 3D model. COLMAP+PMVS required a similar time to compute the 3D point cloud as VisualSFM, as illustrated in Figure 4.

3.3 | Computational Experiment 2: Comparison of three-dimensional trait accuracy with maximal surface density three-dimensional models

The results of the first computational experiment showed that COLMAP produced higher surface density compared to the other tested algorithms, using around 360 images per sample. In the second computational experiment, we tested whether the increased surface density enabled similar trait measurement accuracy using COLMAP with around 600 images, compared to the original version of DIRT/3D (Liu et al., 2021) using 3600 images with VisualSFM. Therefore, we implemented COLMAP in the 3D reconstruction pipeline in DIRT/3D (Liu et al., 2021) and named it DIRT/3D (COLMAP) to distinguish it from the old DIRT/3D (VisualSFM).

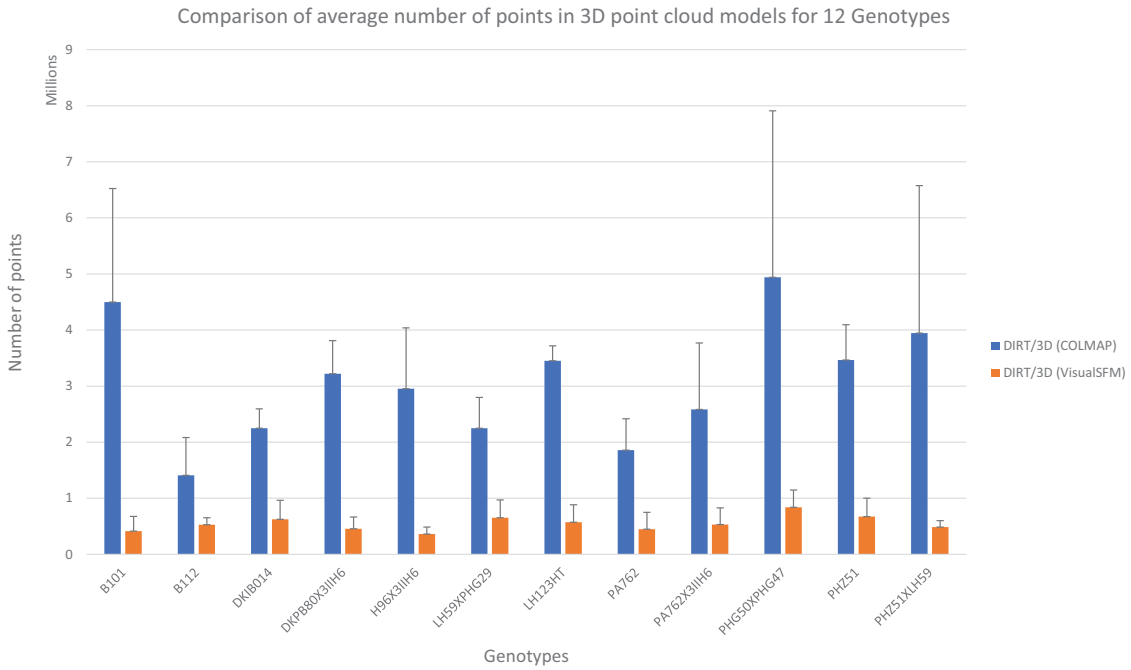

FIGURE 6 Comparison of the number of points in 3D models generated by DIRT/3D (COLMAP) and DIRT/3D (VisualSFM). The average numbers of points for the genotypes are rendered in different color bars. The lengths of the bars represent the value of the number of points. Black lines represent standard deviation.

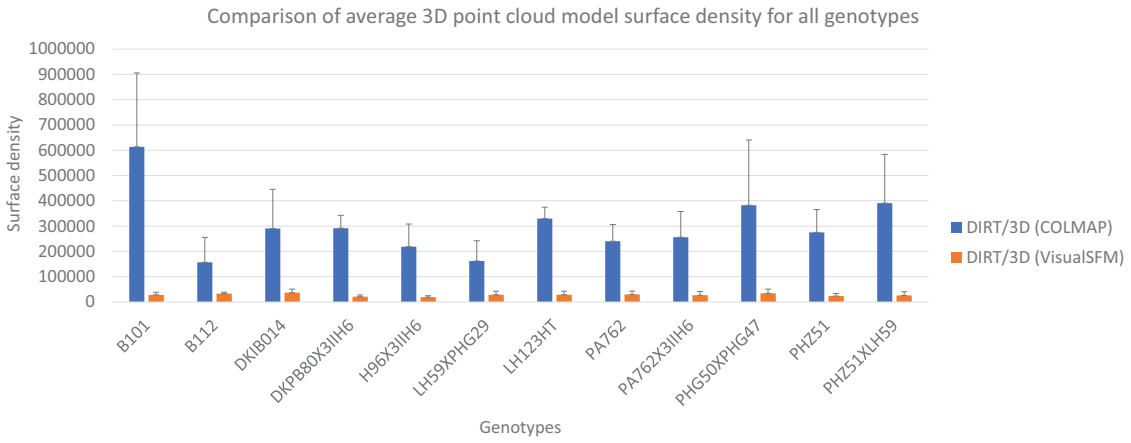

FIGURE 7 Comparison of surface density in 3D models generated from DIRT/3D (COLMAP) and DIRT/3D (VisualSFM). Average surface density for each genotype is rendered in different color bars, with the lengths of the bars representing the value of surface density. Standard deviation is represented as black lines. Surface density is defined as the number of neighbors divided by the neighborhood surface area.

In this computational experiment, we used the maize-root image dataset as described in DIRT/3D (Liu et al., 2021). The full dataset includes 12 genotypes with 5–10 replicates per genotype. For each root sample, we uniformly sampled 600 images from around 3600 images. A visualization of the 12 example 3D root models and their skeletal curves is provided in Figure 5.

We also compared the average number of points for each genotype for all samples within the genotype (Figure 6). The comparison revealed that the number of points generated from DIRT/3D (COLMAP) increased, on average, six times compared with that of DIRT/3D (VisualSFM). The largest increase in the number of points was observed for genotype B101. The average number of points generated by DIRT/3D (COLMAP) was approximately 11 times higher for B101 than in the 3D models generated by DIRT/3D (VisualSFM). The smallest increase in the number of points was observed for genotype LH59 x PHG29; the average number of points increased by about three times when changing from DIRT/3D (VisualSFM) to DIRT/3D (COLMAP).

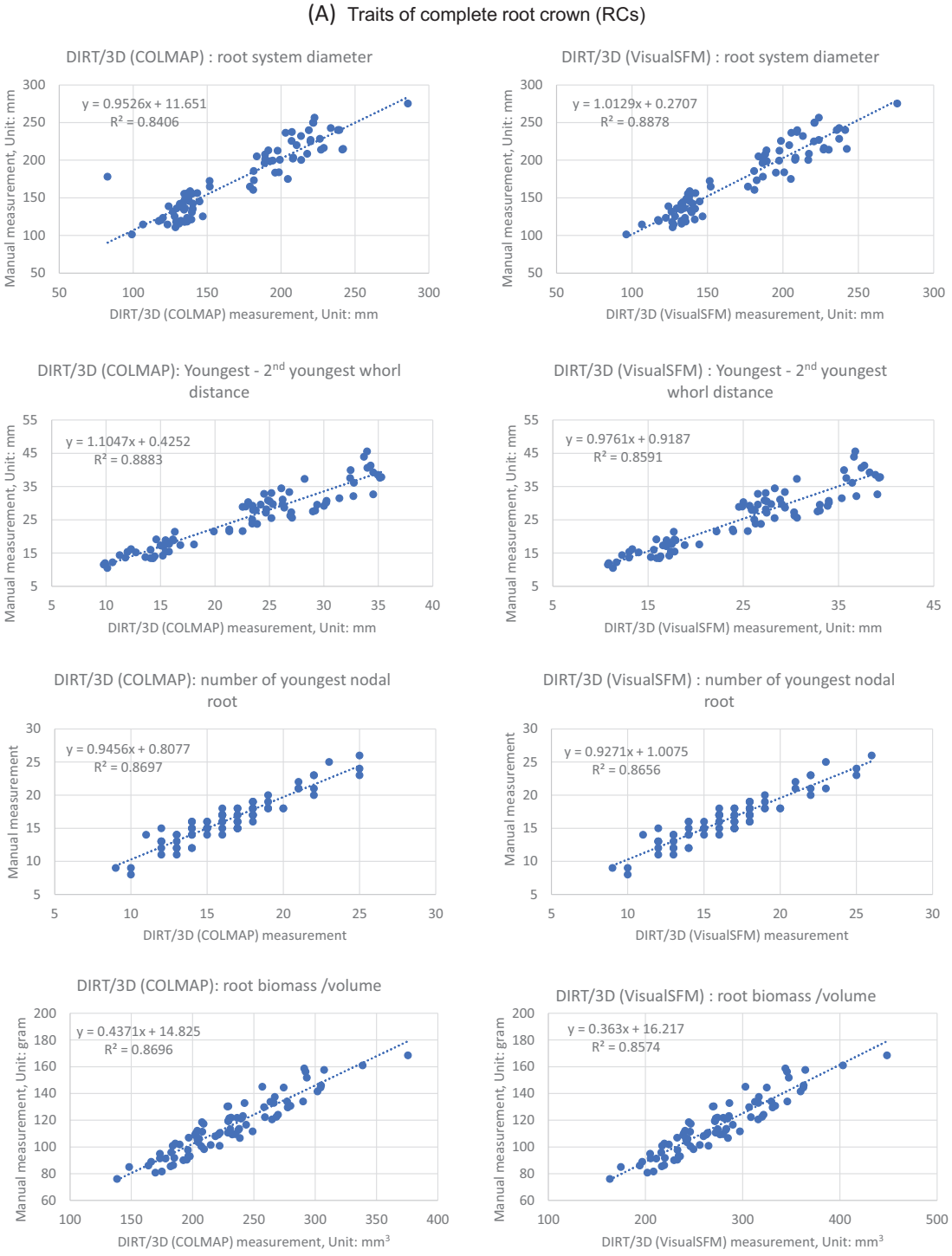

FIGURE 8 Comparison of correlation analysis of 10 traits. Results computed by DIRT/3D (COLMAP) and DIRT/3D (VisualSFM). The *y*-axis represents the manual measurement values, whereas the *x*-axis represents the DIRT/3D (COLMAP) or DIRT/3D (VisualSFM) computed values. R^2 represents R-squared value in regression analysis. The dotted blue lines represent the linear trending lines of the correlation.

In addition to the average number of points, we further compared the surface density of 3D models generated by DIRT/3D (VisualSFM) and DIRT/3D (COLMAP). The results in Figure 7 reveal that the model surface density improvement is significant between DIRT/3D (VisualSFM) and DIRT/3D (COLMAP). The results indicate that the surface density of the 3D model generated by DIRT/3D (COLMAP) increased, on average 11 times compared with that of DIRT/3D (VisualSFM).

The largest increase in surface density was observed for genotype B101, which increased 22 times from the DIRT/3D (VisualSFM) implementation to the DIRT/3D (COLMAP)

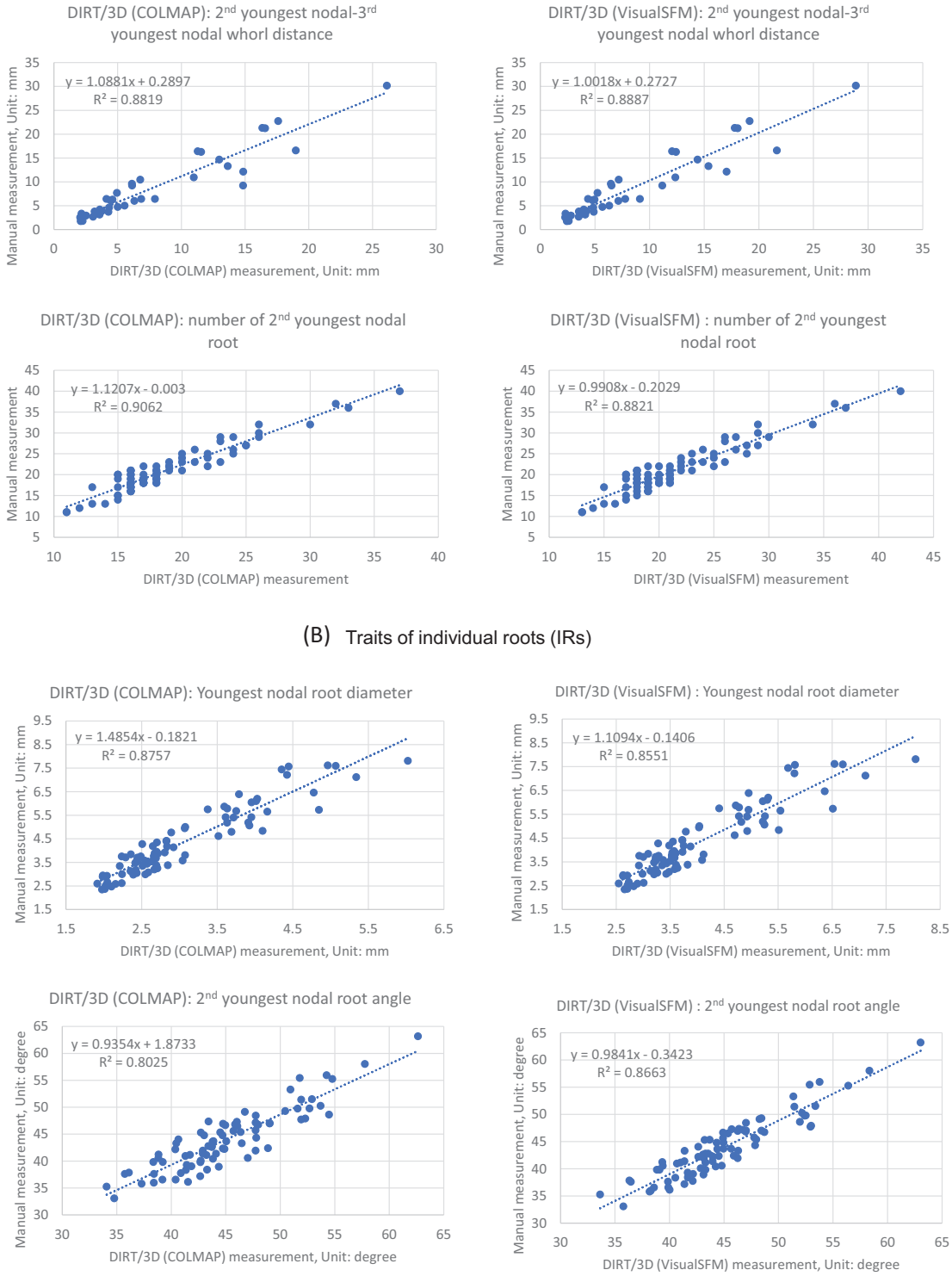

FIGURE 8 Continued

implementation. The smallest increase in surface density was found for genotype B112, which still increased five times.

In our acuracy analysis of traits measurements, we used the manual measurements of ten 3D root traits and compared their correlations with DIRT/3D (VisualSFM) and DIRT/3D (COLMAP) tra. The correlation analysis of these traits revealed $R^2 > 0.80$ and $p < 0.001$ (Figure 8). These traits included complete root crown traits and individual root traits, as described in Liu et al. (2021).

Regarding the complete crown root traits, we observed the improvement of trait measurement correlation for most of

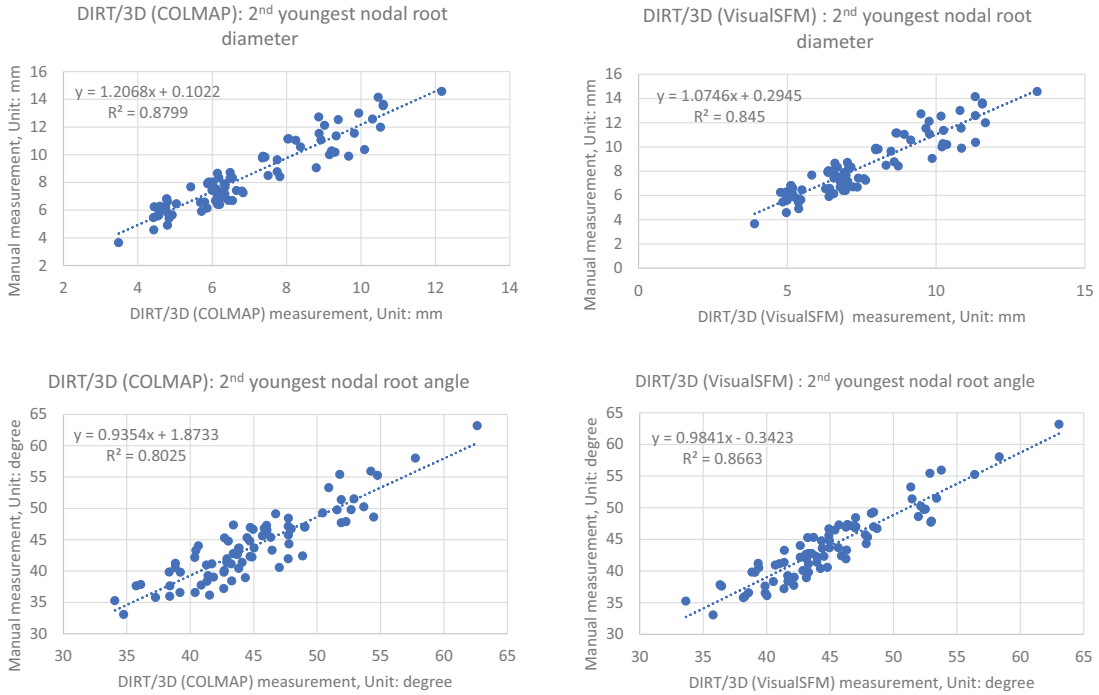

FIGURE 8 Continued

the traits, except root-system diameter and second-youngest nodal–third-youngest nodal whorl distance (Figure 8A).

For individual root traits, we observed an improvement of trait measurement correlation for the youngest nodal root diameter and second-youngest nodal root diameter (Figure 8B). This improvement might benefit from the surface density increase of DIRT/3D (COLMAP) over DIRT/3D (VisualSFM). Of note is that DIRT/3D (VisualSFM) resulted in $R^2 > 0.8$ in the original datasets, with around 3600 images per sample root; however, DIRT/3D (COLMAP) only required around 600 images per sample root, with the correlations improving despite reducing the number of input images.

4 | DISCUSSION AND CONCLUSIONS

The first computational experiment evaluated the 3D reconstruction quality of five open-source pipelines on field grown-maize root systems. All five pipelines produced point clouds as output. We quantified reconstruction quality as the point count and surface density, and we quantified the efficiency of a pipeline as the total computing time. In our evaluation, COLMAP and COLMAP+PMVS generated the largest number of points and the highest surface density. Although the computation time of COLMAP was around 12 times slower than the VisualSFM implementation used in the original DIRT/3D paper (Liu et al., 2021), COLMAP achieved 10 times the number of points and a 94 times higher surface point density.

More important than the measurable quality metric of the point cloud is the correlation of the trait measurement itself. As such we asked: "Does an improvement in 3D model quality benefit the accuracy of root traits measurement?" The obvious increase in surface point density when using COLMAP in Computational Experiment 1 formed the hypothesis that a drastically reduced input image set can produce equally good trait measurements compared with the 3600 input images used in the original VisualSFM implementation of DIRT/3D (VisualSFM). We tested this hypothesis in our second computational experiment by using around 600 images as input to DIRT/3D (COLMAP). We then computed the correlation of the DIRT/3D (COLMAP) traits against the same manual ground truth used in DIRT/3D (VisualSFM). We observed slightly better correlations for the traits extracted with the COLMAP implementation of DIRT/3D (COLMAP) than with DIRT/3D (VisualSFM). On top of the coefficients of determination, we can visually identify highly similar patterns in the correlation with a manual ground truth for DIRT/3D based on VisualSFM and COLMAP (Figure 8).

Overall, our experiments indicate that it is possible to reduce the image-capturing time and trade it against increased computation time without significantly compromising the accuracy of the trait measurement. This finding suggests potential reductions in imaging time and effort, which typically require a trained staff member to place each root in the

3D scanning device manually and wait for the scanning process to finish before placing the next root (Liu et al., 2021). Reducing the number of images from around 3600 to around 600 reduces scanning time from seven minutes to four minutes per root and can reduce data transfer times from the scanner to online storage at CyVerse (Devisetty et al., 2016) from 15 min to 6 min (based on our second experiment). This outcome promises to streamline the most labor-intensive step of the root-phenotyping process.

We found that reductions in scanning and computation time are possible without excessively diminishing model quality. Our results highlight the need for further exploration of tradeoffs in root-image processing and demonstrate that neither customized operating rooms nor highly trained staff are necessary to operate a high-throughput root-imaging system. Our 3D imaging system promises to excel in high-throughput applications as an inexpensive and scalable 3D scanning solution for 3D root phenotyping.

AUTHOR CONTRIBUTIONS

Suxing Liu: Conceptualization, data curation, formal analysis, software, validation, visualization, writing – original draft. **Wesley Paul Bonelli**: Methodology, software, writing – review and editing. **Peter Pietrzyk**: Data curation, methodology, resources, writing – review and editing. **Alexander Bucksch**: Conceptualization, funding acquisition, investigation, methodology, project administration, supervision, writing – review and editing.

ACKNOWLEDGMENTS

This research was supported by the NSF CAREER Award No. 1845760 and USDOE ARPA-E ROOTS Award Number DE-AR0000821 to Alexander Bucksch. Any opinions, findings, and conclusions or recommendations expressed in this material are those of the author(s) and do not necessarily reflect those of the founders. The work was performed during a transition period from the University of Georgia to the University of Arizona.

CONFLICT OF INTEREST STATEMENT

The authors declare no conflicts of interest.

DATA AVAILABILITY STATEMENT

GitHub link for all the scripts for running the test: https://github.com/Computational-Plant-Science/3D_review_scripts/tree/master

https://github.com/Computational-Plant-Science/3D_model_reconstruction_demo

https://github.com/Computational-Plant-Science/3D_model_traits_demo

Permamnent DOI link to access manuscript data on CyVerse Data Commons: https://www.doi.org/10.25739/sg2m-ky55/

ORCID

Suxing Liu https://orcid.org/0000-0001-7639-4470
Wesley Paul Bonelli https://orcid.org/0000-0002-2665-5078
Peter Pietrzyk https://orcid.org/0000-0002-6794-8133
Alexander Bucksch https://orcid.org/0000-0002-1071-5355

REFERENCES

Ault, T. R. (2020). On the essentials of drought in a changing climate. *Science*, *368*(6488), 256–260. https://doi.org/10.1126/science.aaz5492

Bucksch, A. (2014). A practical introduction to skeletons for the plant sciences. *Applications in Plant Sciences*, *2*(8), 1400005.

Bucksch, A., Burridge, J., York, L. M., Das, A., Nord, E., Weitz, J. S., & Lynch, J. P. (2014). Image-based high-throughput field phenotyping of crop roots. *Plant Physiology*, *166*(2), 470–486. https://doi.org/10.1104/pp.114.243519

Clark, R. T., MacCurdy, R. B., Jung, J. K., Shaff, J. E., McCouch, S. R., Aneshansley, D. J., & Kochian, L. V. (2011). Three-dimensional root phenotyping with a novel imaging and software platform. *Plant Physiology*, *156*(2), 455–465.

Delory, B. M., Baudson, C., Brostaux, Y., Lobet, G., Du Jardin, P., Pagès, L., & Delaplace, P. (2016). archiDART: An R package for the automated computation of plant root architectural traits. *Plant and Soil*, *398*(1–2), 351–365.

Devisetty, U. K., Kennedy, K., Sarando, P., Merchant, N., & Lyons, E. (2016). Bringing your tools to CyVerse Discovery Environment using Docker. *F1000Research*, *5*, 1442.

Dowd, T. G., Li, M., Bagnall, G. C., Johnston, A., & Topp, C. N. (2022). Root system architecture and environmental flux analysis in mature crops using 3D root mesocosms. *BioRxiv*, 1–36. https://doi.org/10.1101/2022.09.10.507424

Fuhrmann, S., Langguth, F., & Goesele, M. (2014). *MVE-A multi-view reconstruction environment*. GCH.

Furukawa, Y., & Ponce, J. (2007). Accurate, dense, and robust multi-view stereopsis (PMVS). IEEE Computer Society Conference on Computer Vision and Pattern Recognition.

Galkovskyi, T., Mileyko, Y., Bucksch, A., Moore, B., Symonova, O., Price, C. A., Topp, C. N., Iyer-Pascuzzi, A. S., Zurek, P. R., & Fang, S. (2012). GiA Roots: Software for the high throughput analysis of plant root system architecture. *BMC Plant Biology*, *12*(1), 116.

Girardeau-Montaut, D. (2016). *CloudCompare*. EDF R&D Telecom ParisTech.

Griwodz, C., Gasparini, S., Calvet, L., Gurdjos, P., Castan, F., Maujean, B., De Lillo, G., & Lanthony, Y. (2021). AliceVision Meshroom: An open-source 3D reconstruction pipeline. *Proceedings of the 12th ACM Multimedia Systems Conference*.

Hoppe, C., Klopschitz, M., Rumpler, M., Wendel, A., Kluckner, S., Bischof, H., & Reitmayr, G. (2012). *Online feedback for structure-from-motion image acquisition*. BMVC.

Liu, S., An, P., Zhang, Z., Zhang, Q., Shen, L., & Jiang, G. (2009). On the relationship between multi-view data capturing and quality of rendered virtual view. *The Imaging Science Journal*, *57*(5), 250–259.

Liu, S., Barrow, C. S., Hanlon, M., Lynch, J. P., & Bucksch, A. (2021). DIRT/3D: 3D root phenotyping for field-grown maize (*Zea mays*).

Plant Physiology, *187*(2), 739–757. https://doi.org/10.1093/plphys/kiab311

Lynch, J. P. (2019). Root phenotypes for improved nutrient capture: An underexploited opportunity for global agriculture. *New Phytologist*, *223*(2), 548–564.

Lynch, J. P., & Wojciechowski, T. (2015). Opportunities and challenges in the subsoil: Pathways to deeper rooted crops. *Journal of Experimental Botany*, *66*(8), 2199–2210.

Moulon, P., Monasse, P., Perrot, R., & Marlet, R. (2016). Openmvg: Open multiple view geometry. *International Workshop on Reproducible Research in Pattern Recognition*.

Paustian, K., Agren, G., & Bosatta, E. (1997). Modelling litter quality effects on decomposition and soil organic matter dynamics. *Driven by Nature: Plant Litter Quality and Decomposition*, *1997*, 313–335. https://agris.fao.org/agris-search/search.do?recordID=US201302873310

Schonberger, J. L., & Frahm, J.-M. (2016). Structure-from-motion revisited. *Proceedings of the IEEE Conference on Computer Vision and Pattern Recognition*.

Seethepalli, A., Guo, H., Liu, X., Griffiths, M., Almtarfi, H., Li, Z., Liu, S., Zare, A., Fritschi, F. B., & Blancaflor, E. B. (2020). RhizoVision crown: An integrated hardware and software platform for root crown phenotyping. *Plant Phenomics*, *2020*, 3074916.

Shahzad, Z., Kellermeier, F., Armstrong, E. M., Rogers, S., Lobet, G., Amtmann, A., & Hills, A. (2018). EZ-Root-VIS: A software pipeline for the rapid analysis and visual reconstruction of root system architecture. *Plant Physiology*, *177*(4), 1368–1381.

Shao, M.-R., Jiang, N., Li, M., Howard, A., Lehner, K., Mullen, J., Gunn, S., McKay, J., & Topp, C. (2021). Complementary phenotyping of maize root system architecture by root pulling force and X-ray imaging. *Plant Phenomics*, *2021*, 9859254.

Shi, X., Choi, D., Heinemann, P. H., Hanlon, M., & Lynch, J. (2019). RootRobot: A field-based platform for maize root system architecture phenotyping. *2019 ASABE Annual International Meeting*, Boston, USA.

Smith, P., Martino, D., Cai, Z., Gwary, D., Janzen, H., Kumar, P., McCarl, B., Ogle, S., O'Mara, F., & Rice, C. (2007). Greenhouse gas mitigation in agriculture. *Philosophical Transactions of the Royal Society B: Biological Sciences*, *363*(1492), 789–813.

Topp, C. N., Iyer-Pascuzzi, A. S., Anderson, J. T., Lee, C.-R., Zurek, P. R., Symonova, O., Zheng, Y., Bucksch, A., Mileyko, Y., & Galkovskyi, T. (2013). 3D phenotyping and quantitative trait locus mapping identify core regions of the rice genome controlling root architecture. *Proceedings of the National Academy of Sciences*, *110*(18), E1695–E1704.

van Dusschoten, D., Metzner, R., Kochs, J., Postma, J. A., Pflugfelder, D., Bühler, J., Schurr, U., & Jahnke, S. (2016). Quantitative 3D analysis of plant roots growing in soil using magnetic resonance imaging. *Plant Physiology*, *170*(3), 1176–1188.

Wu, C. (2011). *VisualSFM: A visual structure from motion system*. https://ccwu.me/vsfm/index.html

SUPPORTING INFORMATION

Additional supporting information can be found online in the Supporting Information section at the end of this article.

How to cite this article: Liu, S., Bonelli, W. P., Pietrzyk, P., & Bucksch, A. (2023). Comparison of open-source three-dimensional reconstruction pipelines for maize-root phenotyping. *The Plant Phenome Journal*, *6,* e20068. https://doi.org/10.1002/ppj2.20068